Structural Characterization DNA Binding and Antibacterial Studies of Transition Metal complexes with 2-formylpyridine acetoylhydrazone (FPAH): X-Ray Structure Determination of $Co(FPAH)_2Cl.2H_2O$ Complex

Anuja K., Hussain Reddy K.*, Nagamani Y.B., Srinivasulu K. and Dhanalakshmi D.
Department of Chemistry, Sri Krishnadevaraya University, Ananthapuramu- 515 003, INDIA
*khussainreddy@yahoo.co.in

Abstract

Cobalt(II), nickel(II) and copper(II) complexes with 2-formylpyridine acetoyllhydrazone (FPAH) are synthesized and characterized by elemental analyses, mass spectra, molar conductivity data IR, UV-Vis spectroscopy. The complexes are found to have general formula $M(FPAH)_2$ (where M = Cu(II), Ni(II) and Co(II). Further the copper complex is probed using ESR spectra. The spin Hamiltonian, orbital reduction and bonding parameters are calculated for the complex. The structure of $Co(FPAH)_2Cl.2H_2O$ is determined using single crystal X-ray crystallography. The complex crystallizes in monoclinic space group $P2_1/c$ with a = 11.2702(8) Å, b = 12.0344(9) Å, c = 14.9897(10) Å, α = 90°, β= 106.482(2)°, γ = 90°, 1949.5(2) $Å^3$ and Z = 4 with central Co(II) ion distorted octahedral structure coordinated by two tridentate FPAH ligands.

The interactions of these complexes with calf thymus DNA have been investigated using absorption spectrophotometry. The copper complex binds DNA more strongly than either nickel or cobalt complexes. The ligand and its metal complexes are screened for their antibacterial activity against pathogenic bacterial strains. Complexes showed higher activity than the metal free ligand. Cobalt complex shows more activity than any other two complexes under investigation.

Keywords: Transition Metal complexes, 2-formylpyridine acetoylhydrazone, Spectral characterization, X-Ray crystallography, DNA binding, Antibacterial activity.

Introduction

Heterocyclic compounds are of interest in pharmaceutical chemistry. For example, the drug pralidoxime can be produced from 2-formylpyridine. Niacin is pyridine derivative. Pyridine became an interesting target in 1930 with the importance of niacin for the treatment of dermatitis and dementia[8]. Pyridine derivatives are very important chemicals with tremendous biological application. In medicinal applications, these compounds share an important part. Pyridine derivatives have moderate to excellent activities against number of biological targets. With changing substituent on the pyridine nucleus, the biological targets vary from microbial diseased to viral problems and variety of cancerous cells. Pyridine derivatives target different biological problems by interacting with enzymes, proteins and DNA.

The development of new hydrazone derivatives is an interesting activity of current research. The inspiration stems from their biological activities such as anticonvulsant, antioxidant, hormone antagonist, analgesic, anti-inflammatory, antiplatelet, antimalarial, antimicrobial, antimycobacterial, antitumor, vasodilator, antiviral and antitrypanosomal activities.

Deoxyribonucleic acid (DNA) acts as the main intracellular target for those who thrive to develop a new drug for innumerable diseases especially cancer. It is thought that the pharmaceutical activity of compounds is due to their interaction/ reactions with DNA. Metal complexes have been used as tools for understanding DNA structure, as agents for mediation of DNA or as chemotherapeutic agents. Metal complexes provide an opportunity to explore the effects of central metal atom, the ligands and the coordination geometries on the binding event. Moreover, the activity of complex depends on binding ability to DNA strands [27, 32].

Platinum- based complexes had been primary focus of research on chemotherapy agents[1,2,15]. Since platinum complexes are expensive and show side effects, the interests in this field have shifted to non-platinum based agents. Essential transition metal complexes appear to be very promising agents for anticancer therapy having effective cytotoxic activities. The literature survey indicates that the pharmacological activity depends on the nature of metal ion, organic scaffold and specific DNA binding site[29].

Tridentate hydrazones having assorted donor atoms are efficient ligands in coordinating with metal ions to form complexes having specific geometry. Such complexes serve as models for metallo-proteins containing active sites[12,28,30]. A large number of transition metal complexes of hydrazones have been reported[23] but there are few reports available in the literature on DNA binding of such complexes.

Copper(II) and zinc(II) complexes with 2-benzoylpyridine-methylhydrazone are reported[22] Mn(II), Co(II), Ni(II), Cu(II) and Zn(II) complexes of 2-acetylpyridine benzoylhydrazone were reported[11].

Recently we have reported[9,19,20,32] lanthanide complexes of 2-benzoylpyridine benzoyllhydrazone, 2-actylylpyridine acetoylhydrazone, 2-benzoylpyridine acetoyllhydrazone and 2-formylpyridine benzoylhydrazone. But there is no report on DNA binding studies on transition metal complexes with 2-formylpyridine acetoylhydrazone.

In the light of the above and in continuation of our previous studies,[6,7,17,18] herein we report the synthesis, structural characterization and DNA binding properties of copper(II), nickel(II) and cobalt(II) complexes with 2-formylpyridine acetoylhydrazone (Fig. 1). Single crystal X-Ray structure determination of $Co(FPBH)_2$ complex is reported in this study.

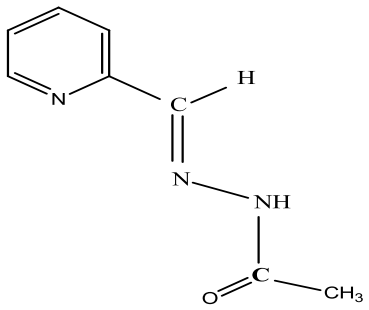

Fig. 1: Structure of 2-formylpyridine acetoylhydrazone

Material and Methods

Chemicals: 2-formylpyridine and acetichydrazide were of reagent grade (Aldrich) and were used without further purification. Metal chloride salts used in the synthesis of complexes were of reagent grade (Merck). Solvents used in the present study were distilled before use. Calf thymus DNA was purchased from Genie Bio labs, Bangalore, India. All other chemicals were of AR grade and used without purification.

Synthesis of ligand and complexes: The ligand was prepared by condensation of a 2-formylpyridine with acetichydrazide in ethanol solvent. 1.48 g of acetichydrazide (20 mmol) dissolved in 30 mL of ethanol were added to ethanolic solution (30 mL) of 2-formylpyridine (20 mmol). The contents were refluxed over water bath for 2hrs and cooled to room temperature. On slow evaporation of solvent, a yellow coloured product was formed. It was collected by filtration, washed with methanol and dried in vacuum. The structures of reactants and product are shown in scheme 1.

The complexes were prepared by mixing hot methanolic (20ml) solution of FPAH (1g, 0.61 mmol) and suitable metal salt ($CoCl_2.6H_2O$/ $NiCl_2.6H_2O$ /$CuCl_2.2H_2O$; 0.61 mmol) dissolved in methanol (20ml) in 1:1 ratio in a clean 100 ml round bottom flask and the contents were refluxed on water bath for 3 hrs and cooled to room temperature. On slow evaporation, coloured complex which separated out was collected by filtration, washed with methanol followed by hexane and dried in vacuuo.

Physical measurements: The conductivity measurements at 298±2 in dry and purified DMF were carried out on CM model 162 conductivity cell (ELICO). ESI-Mass spectral data were obtained from Karunya Institute of Technology and Sciences, Coimbatore, India. The electronic spectra of metal complexes were recorded in DMF with an ELICO spectrophotometer. The infrared spectra were recorded in the range 4000-400 cm^{-1} with Perkin Elmer spectrum 100 spectrometer in KBr discs. ESR spectra were recorded in solid state and in DMF at 298 K and at liquid nitrogen temperature (L.N.T) on a Varian E-112 spectrometer with 100 KHz field modulation. The $g_{\parallel}$ and $g_{\perp}$ values are computed from the spectrum using tetracyanoethylene (TCNE) free radical as 'g' marker.

X-ray Crystallography: X-ray crystallographic data and cell refinement parameters were collected on Enraf Nonius CAD4-MV31 diffractometer, (SAIF-IIT Madras) using graphite monochromated Mo Kα radiation at room temperature 293 K. The data collected were reduced using the SAINT program[26]. The structure was solved by direct method using SHELXS-86 [24] and refined by full-matrix least square on F^2 (SHELXL-97)[25]. The graphic tool used was DIAMOND for windows[3]. ORTEP3[4] was used to generate the ORTEP diagram.

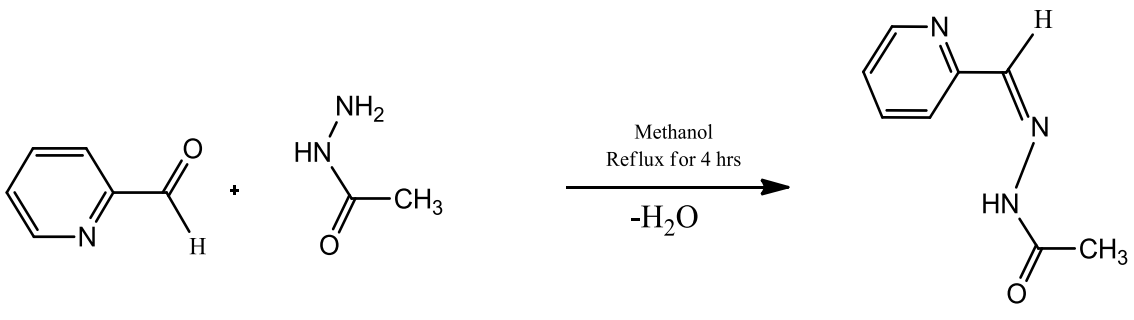

FPAH

Scheme 1: Preparation of 2-formylpyridine acetoylhydrazone (FPAH)

DNA Binding Experiments: DNA binding experiments were done in tris-buffer (0.5mM NaCl/5mM Tris-HCl; pH = 7.0). A solution of CT-DNA in the buffer medium gave a ratio of UV absorbance at 260 and 280 nm (A_{260}/A_{280}) of 1.8-1.9, indicating that the CT-DNA was apparently free of proteins. Concentration of CT-DNA was estimated by using the ε value of 6600 M^{-1} cm^{-1} at 260 nm and stock solution of DNA was always stored at 4ºC. The electronic spectra of metal complexes in aqueous solutions were monitored in the absence and presence of CT-DNA.

Absorption titrations were performed by maintaining the metal complex concentration 10 $x10^{-6}$ M and varying the nucleic acid concentration (0 to7.36 $\times10^{-6}$ M). Absorption titration experiments were performed by varying the concentration of CT-DNA with each addition of 10 µL DNA with the fixed metal complex concentration. The ratio of r = [complex]/[DNA] values varies from 23.41 to 2.60.

Results and Discussion

Characterizations of FPAH: The ligand (FPAH) was easily prepared by reacting 2-formylpyridine with acetichydrazide in high yield (82%). APINH is characterized based on FT-IR, NMR and mass spectral data.

IR spectrum: 3180, 2996, 1664, 1647 cm^{-1} are assigned to $\nu_{(aromatic\ CH)}$, $\nu_{(aliphatic\ CH)}$, $\nu_{(C=O)}$ and $\nu_{(C=N)}$ stretching vibrations respectively.

^{1}H-NMR spectrum: (in DMSO solvent) The peaks at δ (8.63-8.94) (multiplet 4H), δ (7.36-7.62) (multiplet 4H), δ(8.13) (singlet 1H), δ(3.34) (singlet 3 H) are respectively assigned to pyridine, isonicotine, -NH and methyl protons**.** Mass spectrum of FPAH is shown in fig. (1). The spectrum of FPAH does not show peak at (*m/z*) 163 due to molecular ion peak. However, the appearance of peaks at *m/z* 42.99 (≃43) and 120.05 suggest that formation of $COCH_3^+$ and $C_6H_6N_3^+$fragment ions respectively. Formation of these two +ve ions corroborates the synthesis of 2-formypyridine acetoylhydrazone(FPAH).

Characterizations of Complexes: The reaction of FPAH with metal chlorides yielded solid and colored complexes. All the complexes are non-hygroscopic, freely soluble in ethanol and many organic solvents. Physicochemical data of complexes are given in table 1.

Molecular formula $Co(FPAH)_2Cl.\ 2H_2O$ complex is proposed based on X-Ray data. Molar conductivity data of $[Cu(FPAH)_2]$ and $[Ni(FPAH)_2]$ complexes suggest non-electrolytic[5] nature of compounds. However, the cobalt complex shows high molar conductivity 67.7 $\Omega^{-1}cm^2\,mol^{-1}$. The value indicates that the cobalt complex is 1:1 electrolyte in DMF medium.

Electronic spectra: Electronic spectral data of metal complexes are given in table 2. The electronic spectrum of copper complex is dominated by intense charge transfer bands at 29,300 cm^{-1}. The presence of a single d-d band at 12,100 cm^{-1} is assigned to $^2Eg \rightarrow {}^2T_2g$ electronic transition in favour of octahedral structure.

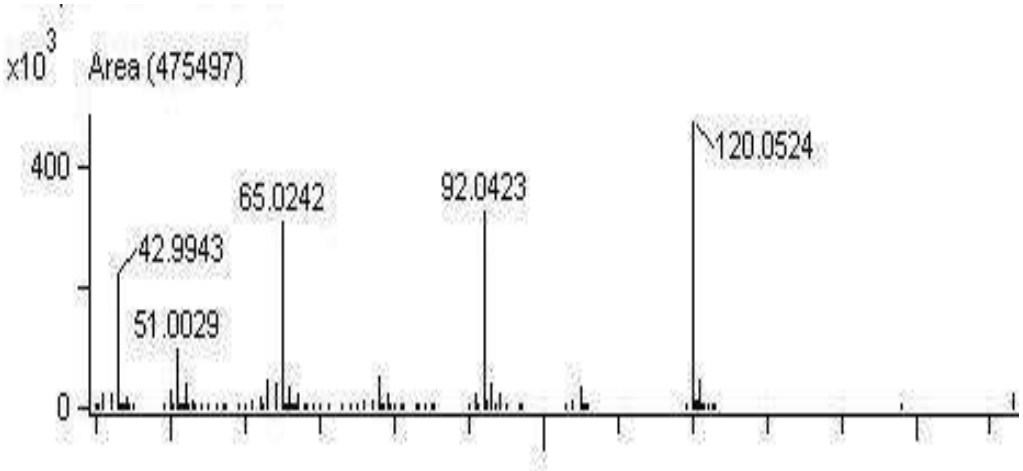

Fig. 1: Mass spectrum of FPAH

Table 1
Physicochemical data of complexes

S. N.	Complex	Colour	Yield %	F. Wt.	Molar Conductivity ($\Omega^{-1}cm^2mol^{-1}$)
1	$[Cu(FPAH)_2]$	Green	80	407.5	10.8
2	$[Ni(FPAH)_2]$	Brown	69	402.7	7.0
3	$[Co(FPAH)_2]Cl.\ H_2O$	Brown	58	454.7	67.7

The electronic spectrum of nickel complex shows bands at 27,900(υ_3), 13,200(υ_2) and 11,000(υ_1) cm^{-1}. These peaks are respectively assigned to ^3A_2g (F) → ^3T_2g(F), ^3A_2g (F) → ^3T_1g(F) and ^3A_2g (F) → $^3T_{12}g$(P) transitions respectively in favour of octahedral structure. The spectral data are utilized to compute important ligand field parameters using ligand field theory of spin allowed transitions in d^8 configuration. The ligand field parameters like field splitting energy (10Dq, 11,000 cm^{-1}), Racah interelectronic repulsion parameters (B', 540 cm^{-1}) and *nephelauxetic* ratio (β, 0.524) and percentage of covalent character (47.6) have been calculated.

The β value is less than unity suggesting considerable amount of covalent character in M─L bond. Electronic spectrum of cobalt complex shows distinct bands at 24,800 and 16,600 cm^{-1}. These peaks are assigned to $^1A_{1g} \rightarrow {}^1T_{1g}$ and $^1A_{1g} \rightarrow {}^1T_{2g}$ transitions respectively in favour of (low-spin) octahedral structure.

IR spectra: IR spectrum of FPAH ligand is compared with spectra of metal complexes to determine donor atoms of ligand. Important IR spectral bands and their assignment are given in table 3.

The IR spectra of the ligands have several prominent bands due to $\nu_{N-H,}$ $\nu_{C=O}$ and $\nu_{C=N}$ stretching modes. The first two bands disappeared in spectra of complexes (due to enolization followed by complexation) and a new ν_{C-O} band appeared around 1020 cm^{-1}. The $\nu_{C=N}$ is shifted to lower (Δυ = 21-22 cm^{-1}) frequency in the spectra of all complexes suggesting the involvement of azomethine nitrogen in chelation. The changes in IR spectra of complexes indicate that the ligand acts as mono anionic tridentate ligand in all the complexes. Based on physicochemical and spectral data, a general structure (fig. 2) is proposed for complexes.

ESR spectra of copper complex: The g values were computed from the spectrum using tetracyanoethylene (TCNE) free radical as the g marker.

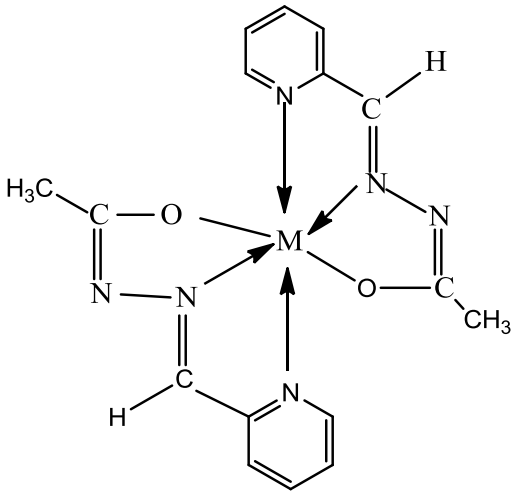

M= Co, Ni, Cu

Fig. 2: Proposed general structure for the complexes

Table 2
Electronic spectral data of metal complexes

Complex	Wavelength λ max (nm)	Wavenumber (cm^{-1})	Assignment
$[Cu(FPAH)_2]$	290	34,500	π - π* Transition
	344	29,300	Charge Transfer Transition
	825	12,100	d-d transition
$[Ni(FPAH)_2]$	278	36,000	**π - π*** Transition
	359	27,900	d-d transition
	757	13,200	d-d transition
	912	11,000	d-d transition
	289	34,600	**π - π*** Transition
$[Co(FPAH)_2]Cl.\ 2H_2O$ 3	373	26,800	Charge Transfer Transition
	601	16,600	d-d transition
	676	14,800	d-d transition

Table 3
Important IR spectral data of metal complexes

FPAH	$[Cu(FPAH)_2]$	$[Ni(FPAH)_2]$	$[Co(FPAH)_2]$	Assignment
			3556	υ_{O-H} of H_2O
3180	--	----	-----	υ_{N-H}
1664	-----	--	--	$\upsilon_{C=O}$
1647	1626	1626	1625	$\upsilon_{C=N}$

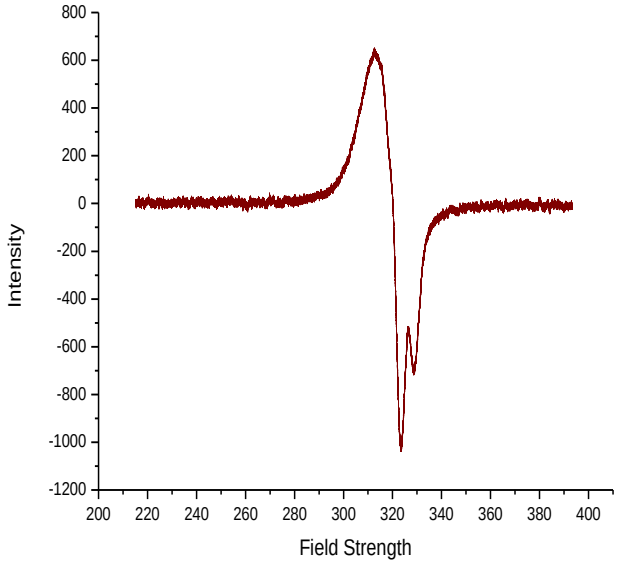

Fig. 3: ESR spectrum of Cu(FPAH)$_2$ complex in DMF at room temperature

Table 4
ESR Data for Cu(FPAH)$_2$ complex

In DMF at RT				In DMF at LNT							
$g_{\parallel}$	$g_{\perp}$	g_{avg}	G	$g_{\parallel}$	$g_{\perp}$	g_{avg}	G	$K_{\parallel}$	$K_{\perp}$	λ	α^2
2.15	2.06	2.09	2.38	2.3	2.05	2.14	6.2	0.99	1.1	489	0.367

At room temperature: ESR spectrum of Cu(FPAH)$_2$ complex in DMF at room nitrogen temperature (RT) is shown in fig. 3. ESR spectral data of complexes in solid state and in DMF are given in table 2. The $g_{\parallel}$ and $g_{\perp}$ values for Cu(FPAH)$_2$ complexes are respectively found to be 2.15 and 2.06 in DMF at room temperature. The $g_{\parallel}$ is less than 2.3 indicating[10] covalent character and value greater than 2.3 shows ionic character of the metal – ligand (M-L) bonding. The $g_{\parallel}$ value suggests covalent character for the complex. The trend, $g_{\parallel} > g_{\perp} > 2.0023$ suggests the unpaired electron predominantly in the $d_{x^2-y^2}$ orbital[10] characteristic of octahedral geometry for copper(II) complex.

The g_{av} value for the complex suggests the presence of covalent character[28] in M-L bond. The axial symmetry parameter *G* is defined as:

$$G = \frac{[g_{\parallel} - 2.0023]}{[g_{\perp} - 2.0023]}$$

The calculated *G* value for Cu(FPAH)$_2$ complex is found to be 2.38. The G value is less than 4 for Cu(FPAH)$_2$ complex which indicates the absence of exchange coupling and misalignment of molecular axes.

At Liquid Nitrogen temperature: The typical ESR spectrum of Cu(FPAH)$_2$ complex in DMF at liquid nitrogen temperature (LNT) is shown in fig. 4. ESR spectra of complexes in DMF at liquid nitrogen temperature (LNT) exhibit well resolved peaks at low field and at high field corresponding to $g_{\parallel}$ and $g_{\perp}$ respectively.

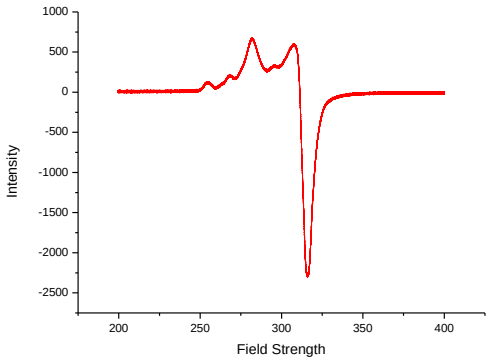

Fig. 4: ESR spectrum of Cu(FPAH)$_2$ complex in DMF at room temperature

The spin Hamiltonian, orbital reduction and bonding parameters of complexes are incorporated in table (4). The $A_{\parallel}$ and $A_{\perp}$ are the separation between two adjacent $g_{\parallel}$ and two adjacent $g_{\perp}$ peaks respectively (in cm^{-1}). The orbital reduction parameters ($K_{\parallel}$, $K_{\perp}$) are calculated and values are incorporated in table 4.

Hathaway pointed for pure sigma bonding $K_{\parallel} = K_{\perp} = 0.77$ and for in-plane pi bonding $K_{\parallel} < K_{\perp}$, while for out-plane π-bonding $K_{\parallel} > K_{\perp}$. These values suggest the presence of in-plane π- bonding in the complex.

The factor α^2, which is usually taken as a measure of covalency is evaluated by the expression:

$$\alpha^2 = A_{\parallel}/ p + (g_{\parallel} -2.0023)3/7(g_{\perp} -2.0023) + 0.004$$

The α^2 value for the complex (0.367) suggests the covalent nature of M-L bond.

Cyclic Voltammetry: Electrochemical properties complexes are revealed by cyclic voltammetry in DMF using 0.1 M tetrabutylammonium hexafluorophosphate as supporting electrolyte. The cyclic voltammogram of copper(II) complex is shown in fig. 5 and the electrochemical data of compounds are summarized in table 5.

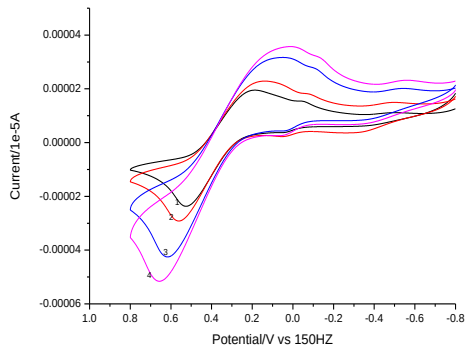

Fig. 5: Cyclic voltammogram of $Cu(FPAH)_2$ complex at different scan rates

It has been observed that cathodic (Ipc) and anodic (Ipa) peak currents were not equal. It may be inferred that cobalt complex undergoes reduction from Co(III) →Co(II) while the bivalent metal(Ni and Cu) derivatives undergo one electron reduction from M(II)→M(I). The non-equivalent current in cathodic and anodic peaks indicates quasi-reversible behavior. The ΔEp values of compounds are better than the Nerstian requirement 59/n mV, which demonstrate quasi-reversible nature of electron transfer. The complexes show high difference between cathodic and anodic peaks indicating quasi-reversible nature.

X-ray structure determination of $Co(FPAH)_2Cl.2H_2O$ complex: The complex, $Co(FPAH)_2Cl.2H_2O$ crystallizes in monoclinic, space group P21/c. The structure refinement parameters are summarized in table 6. Important bond distances and bond angles are given in table 7. ORTEP diagram of the complex is shown in fig. 6. The complex has 6-coordinate cobalt. The structure of complex consists of two monoanionic tridentate FPAH ligands in which Co(III) ion located on the two fold symmetry axis.

The two ligand molecules coordinate the Co(III) ion to form four five membered chelate rings; [Co-O_1-C_7-N_2-N_3; Co-N_3-C_6-C_5-N_1; Co-O_2-C_{15}-N_5-N_6; Co-N_6-C_{14}-C_{13}-N_4]. The two ligands coordinated to the cobalt metal centre are nearly orthogonal [Fig. 6] to each other. The equatorial plane of Co octahedron is defined by two acetyl pyridine ring nitrogen atoms and two oxygen atoms, while the axial positions are occupied by azomethine nitrogen atoms of each ligand molecule. This CoN_4O_2 coordination sphere is considerably distorted, which is probably due to the rigidity of the ligand because of extended conjugation.

The angles at the Co center show large deviation (Table 5) from ideal octahedral values of 90° and 180°. The tridentate ligand in the complex is almost planar. The three individual rings, namely the formylpyridine and the two five membered chelate rings, are individually nearly planar.

The average bond distances for each Co-O and Co-N in this coordination geometry are 1.9045 and 1.8895 Å respectively. The values are similar to that of typical Co(III) complexes. In Co(III) compounds, the expected interatomic Co-O/ Co-N bond lengths are around 1.9 Å whereas in Co(II) compounds the same bond lengths should be around 2.1 Å. Hence bond length data also indicates that metal ion is in + 3 oxidation state.

Equatorial Co-N (formylpyridine)) bond lengths are longer than axial Ni-N (>C=N- moiety) bond lengths, which can be related to greater trans influence of coordinated azomethine nitrogen moiety. The X-Ray crystal data confirm that the complex has distorted octahedral structure (Fig. 6).

Table 5
CV data of metal complexes

Complex	C_v cathodic	C_v anodic	ΔEp (mV)	$E_{1/2}$	$-i_c/i_a$	Log Kc^a	$-\Delta G^{\circ b}$
	E_{pc}	E_{pa}					
$Co(FPAH)_2Cl.2H_2O$	0.188	0.523	711	0.355	0.835	0.047	271
$Ni(FPAH)_2$	-1.103	-0.794	309	0.154	0.026	0.108	623
$Cu(FPAH)_2$	-0.999	-0.789	209	0.014	0.631	0.069	400

[a]log $K_c = 0.434ZF/RT\Delta E_p$; [b]$\Delta G^o = -2.303RTlog$

Table 6
Crystal data* and structure refinement for Cobalt(III) Complex.

S.N.	Parameter	Crystal data	S.N.	Parameter	Crystal data
1	Empirical formula	C_{16} H_{20} Cl Co N_6 O_4	14	Reflections collected	32201
2	Formula weight	454.76	15	Indepen. reflections	3419 [R(int) = 0.0315]
3	Wavelength	0.71073Å	16	Completeness to theta = 24.996	99.6 %
4	Crystal system	Monoclinic	17	Absorption correction	Semi-empirical
5	Space group	$P2_1/c$	18	Max. and min. transmission	0.7453 and 0.6163
6	Volume	1949.5(2) $Å^3$	19	Refinement method	Full-matrix least-squares on F^2
7	Z	4	20	Data / restraints / parameters	3419 / 7 / 265
8	Density (calculated)	1.549 Mg/m^3	21	Goodness-of-fit on F^2	1.137
9	Absorp. coefficient	1.053 mm^{-1}	22	Final R indices [I>2sigma(I)]	R1 = 0.0541, wR2 = 0.1281
10	F(000)	936	23	R indices (all data)	R1 = 0.0659, wR2 = 0.1410
11	Crystal size, mm^3	0.200 x 0.150 x 0.150	24	Extinction coefficient	N/A
12	Theta range	3.153 to 24.996°	25	Largest diff. peak and hole	0.620 and -0.975 $e.Å^{-3}$
13	Index ranges	-13<=h<=13, -14<=k<=14, -17<=l<=17	26		

*Unit cell dimensions; a = 11.2702(8) Å; b = 12.0344(9) Å; c = 14.9897(10) Å; □= 90°; □= 106.482(2)°; □ = 90°.

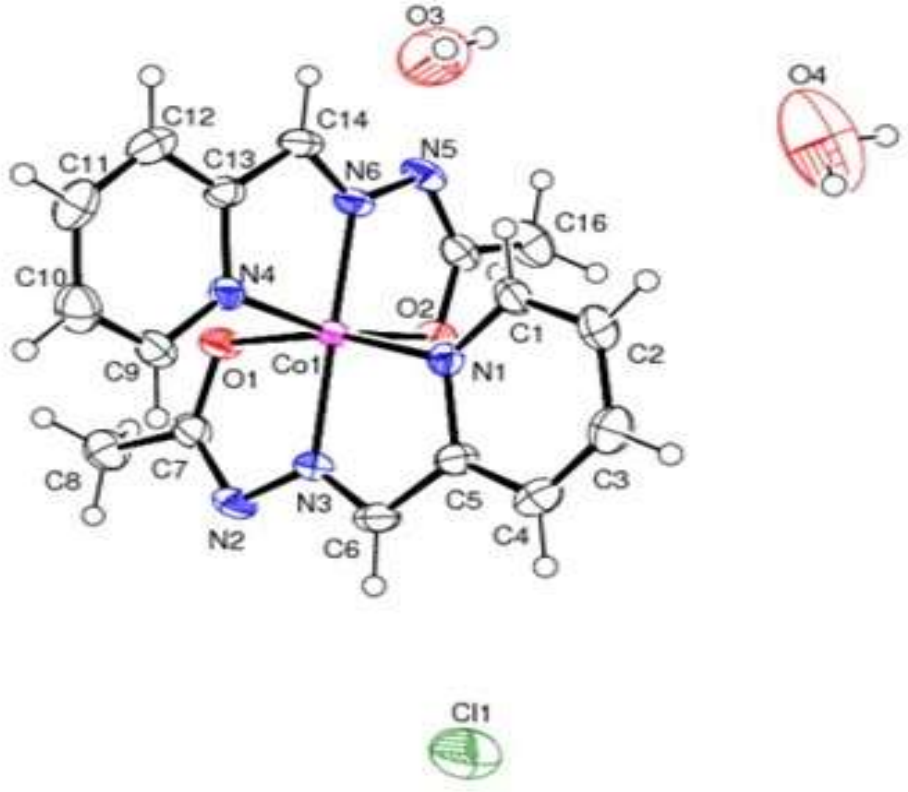

Fig. 6: ORTEP view of $Co(FPAH)_2Cl.2H_2O$ complex

Table 7
Bond lengths [Å] and angles [°] for $Co(FPAH)_2Cl.2H_2O$ complex

Type of Bond	Bond length		Type of Angle	Bond Angle	Type of Angle	Bond Angle
Co(1)-N(6)	1.855(3)		N(6)-Co(1)-N(3)	176.78(14)	O(1)-Co(1)-N(4)	90.28(12)
Co(1)-O(2)	1.905(3)		N(6)-Co(1)-O(2)	82.11(13)	N(6)-Co(1)-N(1)	98.53(13)
Co(1)-O(1)	1.904(3)		N(3)-Co(1)-O(2)	95.06(13)	N(3)-Co(1)-N(1)	83.01(14)
Co(1)-N(4)	1.922(3)		N(6)-Co(1)-O(1)	96.35(12)	O(2)-Co(1)-N(1)	91.06(12)
Co(1)-N(1)	1.929(3)		N(3)-Co(1)-O(1)	82.11(13)	O(1)-Co(1)-N(1)	165.11(13)
C(15)-O(2)	1.303(5)		O(2)-Co(1)-O(1)	90.58(12)	N(4)-Co(1)-N(1)	91.88(13)
C(7)-O(1)	1.295(5)		N(6)-Co(1)-N(4)	83.16(14)		
N(2)-N(3)	1.384(5)		N(3)-Co(1)-N(4)	99.65(14)		
N(5)-N(6)	1.373(4)		O(2)-Co(1)-N(4)	165.24(13)		
Co(1)-N(6)	1.852(3)					

Table 8
Hydrogen bonds for $Co(FPAH)_2Cl.2H_2O$ complex [Å and °].

D-H...A	d(D-H)	d(H...A)	d(D...A)	<(DHA)
C(4)-H(4)...Cl(1)	0.93	2.64	3.492(5)	152.5
C(6)-H(6)...Cl(1)	0.93	2.92	3.674(5)	138.7
C(8)-H(8B)...Cl(1)#1	0.96	2.70	3.642(6)	166.6
C(9)-H(9)...N(2)#1	0.93	2.50	3.321(5)	147.1
C(12)-H(12)...O(1)#2	0.93	2.52	3.303(5)	141.9
C(14)-H(14)...Cl(1)#3	0.93	2.74	3.539(4)	144.2
O(3)-H(3A)...O(3)#4	0.81(2)	2.506(12)	3.008(9)	121.1(12)
O(3)-H(3B)...Cl(1)#3	0.83(2)	2.50(10)	2.939(7)	114(9)
O(4)-H(4B)...Cl(1)#5	0.86(2)	2.35(4)	3.193(8)	164(9)

Symmetry transformations used to generate equivalent atoms:
#1 -x,-y+1,-z+1 #2 -x+1,-y+1,-z+1 #3 x+1,y,z
#4 -x+1,-y,-z+1 #5 -x,y-1/2,-z+1/2

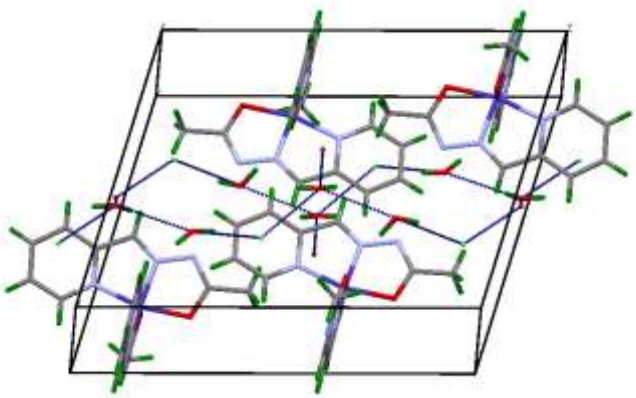

Fig. 7: Packing of the molecule showing non-covalent interactions.

The relatively short $N_2 – N_3$ (1.364 Å) and N_5- N_6 (1.373 Å) bond lengths (normal single bond length is 1.52 Å coupled with lengthened C ─ O distance[C_7-O_1 (1.295 Å ; C_{15}- O_2 1.303 Å] indicate that the ligand binds cobalt in *enol* form. The ketonic [>C=O] bond length is 1.23 Å.

Hydrogen bonding data for the structure of Co(III) complex [Å and °] are given in table 8. Fig. 7 shows packing of the molecule indicating non-covalent interactions.

DNA binding studies: UV- V is spectroscopy is an important technique to investigate the interaction of DNA with metal complexes. Hence the interaction of metal complexes with calf-thymus DNA was monitored by UV-visible spectroscopy. Absorption spectra were recorded in the range of 250-500 nm. Typical absorption spectra in presence and in absence of DNA are shown in fig. 8. Metal complexes exhibit an intense absorption band in high energy region (290- 360 nm) which are attributed to metal-ligand

charge transfer (MLCT) transitions. The absorption spectra of complexes were compared in the absence and in the presence of CT-DNA. The change in absorbance values with increasing amounts of CT-DNA was used to evaluate the intrinsic binding constant Kb, for the complexes. Based on the variation in absorption, the intrinsic binding constant or association constant (K_b) of the metal complex can be calculated according to the Benesi-Hildebrand equation modified by Wolfe et al[31].

$$[DNA]/(\varepsilon_a-\varepsilon_f) = [DNA]/(\varepsilon_b-\varepsilon_f) + 1/Kb\ (\varepsilon_b-\varepsilon_f)$$

where ε_a, ε_f and ε_b correspond to $A_{observed}$ /[complex], the extinction coefficient for the free metal complex and the extinction coefficient for the metal complex fully bound to DNA respectively Kb represents the binding constant.

Electronic absorption spectral data upon addition of CT-DNA and binding constants of these complexes are given in the table 9. In the presence of increasing amounts of CT-DNA, the UV-visible absorption spectra of metal complexes show a small (λmax: 0.5-1.0 nm) with increasing amounts of DNA. The calculated binding constants are found in the range 2.5 - 4.4 x 10^5 M^{-1}.

Such small shifts and lower Kb values are more in keeping with groove binding, leading to small perturbations. The Kb values here are lower than that reported for classical intercalator for ethidium bromide and $[Ru(Phen)_2DPPZ]^{2+}$ complex whose binding constants have been found[13, 14] to be in the order 10^6 - 10^7. The observed binding constants for the present complexes are in accordance with groove binding with DNA as reported in the literature. It is pertinent to note that the binding constant for $Cu(FPBH)_2$ complex is quite high. The increasing order of binding constant is found as shown below:

$Co(FPAH)_2$ < $Ni(FPAH)_2$ < $Cu(FPAH)_2$

The above order suggests that the $Cu(FPAH)_2$ complexes binds DNA strongly.

Antibacterial activity studies: The ligand and its metal complexes are screened for their antibacterial activity by using agar well diffusion method against pathogenic bacterial strains such as *E. coli, K. pneumonia, S. aureus* and *B.cereus* . Inhibition zones are determined in the presence of different amounts (100, 200 and 300 µg/well) of complexes with reference to the positive control *viz*. ciprofloxacin. The diameters of inhibition of zone were measured with Vernier callipers in mm and its values are depicted in the table 10.

Metal complexes exhibited higher antibacterial activity than the metal free ligand in all the cases in analogy with our previous observations[16].

Conclusion

Copper(II), nickel(II) and cobalt(II) complexes of 2-formylpyridine acetoylhydrazone (FPAH) are synthesized and characterized based on physicochemical and spectral data. The cobalt complex is structurally characterized using single crystal X-ray crystallography. The complex is found to have distorted octahedral structure with the central Co(III) ion covalently bound by one chloride ligand and coordinated by two tridentate FPAH ligands.

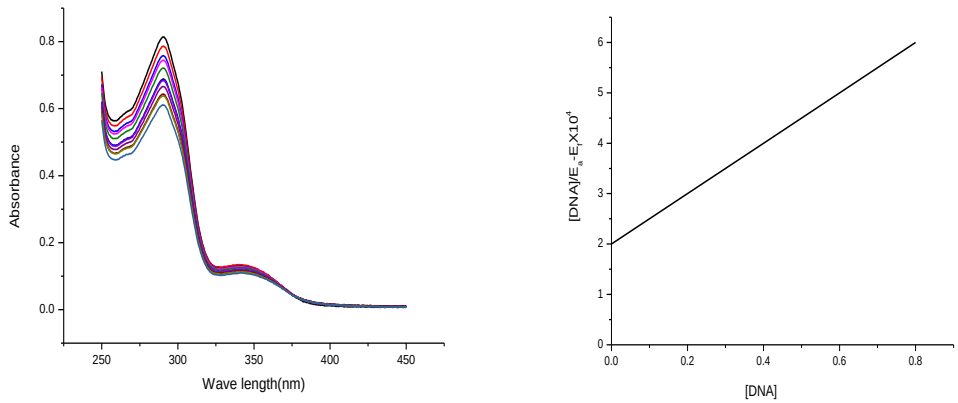

Fig. 8: Absorption spectra of in the absence and in the presence of increasing concentration of CT-DNA.

Table 9
Electronic Absorption Data upon addition of C T –DNA to the Complex

S.N.	Complexes	λ max (nm)		Δ λ	H%	K_b [M^{-1}]
		Free	Bound			
1	$Co(FPAH)_2Cl.2H_2O$	290.0	290.5	0.5	+17.37	$2.5X10^5$
2	$Ni(FPAH)_2$	359.5	359.0	0.5	+9.48	$3.0X10^5$
3	$Cu(FPAH)_2$	359.5	358.5	1.0	+9.20	$4.4X10^5$

Table 10
Antibacterial activity of Metal Complexes against pathogenic bacterial strains

Complex	Treatment	*E. coli*	K.pneumoniae	*S. aureus*	B.cereus
S-Ciprofloxacin	5µg/µL	10.5±0.3	9.8±0.17	10.03±0.15	12.16±0.16
FPAH	100µg/µL	0.8±0.15	0.9±0.25	0.7±0.09	0.7±0.09
	200µg/µL	1.0±0.17	1.0±0.25	0.85±0.31	0.85±0.3
	300µg/µL	1.2±0.25	1.2±0.3	1.0±0.09	1.0±0.25
Co(FPAH)2	100µg/µL	2.9±0.00	2.8±0.09	2.9±0.09	3.0±0.3
	200µg/µL	3.0±0.30	3.6±0.17	3.1±0.00	3.1±0.09
	300µg/µL	3.2±0.25	3.8±0.15	3.5±0.25	3.3±0.00
Ni(FPAH)2	100µg/µL	2.3±0.31	2.2±0.31	1.6±0.25	1.5±0.17
	200µg/µL	2.3±0.09	2.3±0.25	1.8±0.3	1.6±0.17
	300µg/µL	2.5±0.25	2.4±0.30	2±0.25	1.9±0.00
Cu(FPAH)2	100µg/µL	2.1±0.00	2.0±0.17	2.1±0.09	2.3±0.17
	200µg/µL	2.3±0.00	2.1±0.31	2.4±0.3	2.5±0.25
	300µg/µL	2.5±0.09	2.2±0.25	2.6±0.25	2.5±0.3

Values are the mean ± SE (Standard Error) of inhibition zone in mm

The copper complex is investigated using ESR spectra. Groove binding of complexes to DNA is suggested based on binding constants and the variations in the absorption spectra of metal complexes in the presence of DNA.

Acknowledgement

KHR is thankful to UGC for the award of UGC-BSR Faculty Fellowship. The authors also thank UGC and DST for providing equipment facility under SAP and FIST programs respectively. The authors also thank SAIF, IIT-M, Chennai for providing X-ray data of $Co(FPAH)_2Cl.2H_2O$ complex and Karunya Institute of Technology and Sciences, Coimbatore for sending ESI-Mass spectral data. The authors thank Dr. M. Nethaji, Department of Inorganic Physical Chemistry, Indian Institute of Science for giving suggestions in X-Ray crystal structure.

References

1. Abu-Surrah A.S. and Kettunen M., Platinum Group Antitumor Chemistry: Design and development of New Anticancer Drugs Complementary to Cisplatin, *Cur. Med. Chem*., **13**, 1337-1357 **(2006)**

2. Allardyce C.S. and Dyson P.J., Ruthenium in Medicine: Current Clinical Uses and Future Prospects, *Platinum Met. Rev*., **45**, 62–69 (2001)

3. Brandenburg K. and Putz H., DIAMOND version 3.0 Crystal Impact, GbR, Postfach 1251, D-53002, Bonn, Germany **(2004)**

4. Farrugia L.J., ORTEP-3 for windows- a version of ORTEP-III with a graphia user interphase, *J. Appl. Crystallogr.,* **30**, 565- 565 **(1997)**

5. Geary W.J., The use of conductivity measurements in organic solvents for the characterization of coordination compounds, *Coord. Chem. Rev*., **7**, 81-122 **(1971)**

6. Hari Babu P., Patil Y.K., Hussain Reddy K. and Nethaji M., Synthesis, crystal structure, DNA interaction and cleavage activities of mononuclear and trinuclear copper(II) complexes, *Transition Metal Chemistry*, **39,** 167-175 **(2014)**

7. Hari Babu P., Patil Y.K., Hussain Reddy K. and Nethaji M., Novel hexanuclear distorted open-cubane copper complex containing oximato bridges: Synthesis, crystal structure, DNA binding and cleaqvage activity, *Inorg. Chim. Acta*, **392**, 478 -484 **(2012)**

8. Henry G.D., Synthesis of Substituted Pyridines, *Tetrahedron*, **60,** 6043-606 **(2004)**

9. Hussain Reddy K., Raja K. and Suseelamma A., Synthesis, crystal structure, DNA binding and cleavage activity of butterfly-like 12-coordinate praseodymium(III) complex, *Inorganic Nano-Metal Chemistry*, **47**, 1398-1405 **(2017)**

10. Hussain Reddy K., Sambasiva Reddy P. and Babu P.R., Synthesis, spectral studies and nuclease activity of mixed ligand copper (II) complexes of heteroaromatic semicarbazones/thiosemi carbazones and pyridine, *J. Inorg. Biochem*, **77**, 169- 176 **(1999)**

11. Jang Y.J., Lee U.K. and Koo B.K., Synthesis and Crystal Structures of Mn(II), Co(II), Ni(II), Cu(II) and Zn(II) Metal Complexes with NNO Functionalized Ligands, *Bull. Korean Chem. Soc*., **26**, 925- 929 **(2005)**

12. Kitajima N. and Moro-oka Y., Copper-Dioxygen Complexes. Inorganic and Bioinorganic Perspectives, *Chem. Rev*., **94**, 737- 757 **(1994)**

13. Krishnanoorthy P. and Okay O., Evaluation of DNA binding, DNA cleavage, protein binding and *in vitro* cytotoxic activities of bivalent transition metal hydrazone complexes, *Eur J Med. Chem.*, **46**, 3376-3387 **(2011)**

14. Kumar P., Gorai I., Santra M.K., Mandal B. and Manna D., DNA binding, nuclease activity and cytotoxicity studies of Cu (II) complexes of tridentate ligands, *Dalton Trans.,* **41**, 7573-7581 **(2012)**

15. Lippert B., Cis-platin: Chemistry and Biochemistry of a leading Anticancer Drug, Wiley Interscience,183 **(1999)**

16. Moksharagni B., Rishitha M. and Hussain Reddy K., Synthesis, DNA binding properties and antibacterial activity of lanthanide

complexes with 2-benzoylpyridine isonicotinoylhydrazone, *Indian J. Chem*., **56A,** 232-237 **(2017)**

17. Pragathi M. and Hussain Reddy K., Synthesis, spectral characterization and DNA interactions of copper(II) and nickel(II) complexes with unsymmetrical Schiff base ligands, *Indian J. Chem*., **52A**, 845-853 **(2013)**

18. Pragathi M. and Hussain Reddy K., Synthesis, crystal structures, DNA binding and cleavage activity of water soluble mono and dinuclear copper(II) complexes with tridentate ligands, *Inorg. Chim. Acta*, **413**, 174-186 **(2014)**

19. Raja K., Suseelamma A. and Hussain Reddy K., Synthesis, X-ray crystal structure, DNA binding and Nuclease activity of lanthanide(III) complexes of 2-benzoylpyridine acetylhydrazone, *Journal of Chemical Sciences*, **128**, 1265-1275 **(2016)**

20. Raja K., Suseelamma A. and Hussain Reddy K., Synthesis, spectral properties and DNA binding and nuclease activity of lanthanide (III) complexes of 2-benzoylpyridine benzhydrazone: X-ray crystal structure, Hirshfeld studies and nitrate-π interactions of cerium(III) complex, *Journal of Chemical Sciences*, **128**, 23-35 **(2016)**

21. Raja K., Suseelamma A. and Hussain Reddy K., Synthesis, spectral properties, DNA binding interactions and DNA cleavage studies of lanthanide (III) complexes of 2-acetylpyridine acetoylhydrazone: the X-ray crystal structure of 10-coordinate Ce (III) and Sm (III) complexes, *Journal of the Iranian Chemical Society*, **12**, 1473-1486 **(2015)**

22. Recio Despaigne A.A., Da Silva J.G., Do Carmo A.C.M., Piro O.E., Castellano E.E. and Beraldo H., Copper(II) and zinc(II) complexes with 2-benzoylpyridine-methyl hydrazone, *J. Mol. Struct*., **920**, 97-102 **(2009)**

23. Shakdofa M.M.E., Shtaiwi M.H., Morsy N. and Abdel-rassel T.M.A., Metal complexes of hydrazones and their biological, analytical and catalytic applications: A review, *Main Group Chemistry*, **13**, 187–218 **(2014)**

24. Sheldrick G.M., Phase annealing in SHLEX-90: Direct methods for larger structures, *Acta Cryst. A*, **46**, 467 **(1990)**

25. Sheldrick G.M., SHELXS-97 Program for the Solution of Crystal Structures, University of Gottingen, Germany **(1997)**

26. Siemens SMART SAINT, Area detector Control and Integration Software, Simens X-ray Instruments Inc., Madison **(1996)**

27. Shimizu S., Watanabe N., Kataoka T., Shoji T., Abe N., Morishita S. and Ichimura H., Pyridine and Pyridine Derivatives, Ullmann's Encyclopedia of Industrial Chemistry, Weinheim, Wiley-VCH **(2000)**

28. Solomon E.J., Sundaram U.M. and Machonkin T.E., Multicopper Oxidases and Oxygenases, *Chem. Rev*., **96**, 2563-2605 **(1996)**

29. Tabassum S., Zaki M., Arjmand F. and Ahmad I., Synthesis of heterobimetallic complexes: In vitro DNA binding, cleavage and antimicrobial studies, *J. Photochem. Photobiol. B,* **114**, 108-118 **(2012)**

30. Tolman W.B., Making and Breaking the Dioxygen O-O Bond: New Insights from Studies of Synthetic Copper Complexes, *Acc. Chem. Res*., **30**, 227- 237 **(1997)**

31. Wolfe A., Shimer G.H. and Meehan T., Polycyclic aromatic hydrocarbons physically intercalate into duplex regions of denatured DNA, *Biochemistry*, **26**, 6392- 6396 **(1987)**

32. Zeng Y.B., Yang N., Liu W.S. and Tang N., Synthesis, characterization and DNA-binding properties of La(III) complex of chrysin, *J. Inorg. Biochem*., **97**, 258-264 **(2003)**.

(Received 27th October 2020, accepted 28th November 2020)